



## Microstructure & Tribological Performance of Alumina-3wt% Titania Coatings Produced by APS

Mokhtar DJENDEL<sup>1,2\*</sup>, Omar ALLAOU<sup>2</sup>, Mourad MAAZOUZ<sup>3</sup>, Rabah BOUBAAYA<sup>1,2</sup>

<sup>1</sup> Department of Science and Technics, Faculty of Technology, University of Bordj Bou Arreridj, Algeria

<sup>2</sup> Process Engineering Laboratory, University of Laghouat, BP 37G, Laghouat, Algeria.

<sup>3</sup> Departement of Mechanical Engineering, Faculty of Technologies, University of M'Sila, BP 166, M'Sila, Algeria

\* Corresponding Author : [m.djendel@lagh-univ.dz](mailto:m.djendel@lagh-univ.dz) or [djendelm@gmail.com](mailto:djendelm@gmail.com)

ORCID: 0000-0002-8175-6744

### Article Info:

DOI: 10.22399/ijcesen.665097

Received : 26 December 2019

Accepted : 14 May 2020

### Keywords

Plasma spray  
Alumina-3wt.% Titania Coatings  
Microstructure  
XRD, SEM  
Wear behavior.

### Abstract:

Al<sub>2</sub>O<sub>3</sub>-3wt%TiO<sub>2</sub> coatings were deposited by atmospheric plasma spraying (APS). The microstructure and phase composition of the coatings were characterized by X-ray diffraction (XRD) and scanning electron microscopy (SEM). The wear and friction properties of Alumina-3wt.% titania coatings against a steel ball under dry friction conditions were examined. The microstructure result and the phase of the spray coating is analyzed and presented. In addition, wear behavior of the sprayed coating are evaluated for final coating performance. , test results showed that increasing some process parameters increased the performance of mechanical properties of coating and gave the lowest friction coefficient value of coating.

## 1. Introduction

Plasma-sprayed ceramic coatings such as Al<sub>2</sub>O<sub>3</sub>-TiO<sub>2</sub> coatings have been widely applied to structural materials and various machine parts in order to improve resistances to wear, corrosion, oxidization, erosion, and heat [1,2,3]. Plasma Thermal spraying techniques are coating processes in which melted or heated materials are sprayed onto a surface. Thermal spray coatings have a wide range of applications, for instance, by repairing machine parts damaged in service or by the production of parts with high wear resistance [4,5,6]. The Atmospheric Plasma Spraying (APS) is one of these processes. Plasma sprayed alumina-titania ceramic is one of the materials largely used in the APS process [7]. It is known for its wear, corrosion, and erosion resistance applications. In order to advance understanding the relationships between the microstructure and wear resistance of the plasma-sprayed coatings, an Al<sub>2</sub>O<sub>3</sub>-3wt% TiO<sub>2</sub> coating was prepared by plasma spraying and its tribological behaviors against a steel ball under dry conditions was examined.

## 2. Experimental procedure

### 2.1. Materials & coating deposition

An atmospheric plasma spraying system (Sulzer-Metco 9MC equipment) was used to deposit the Al<sub>2</sub>O<sub>3</sub>-3%wt TiO<sub>2</sub> coatings. Using two powder feeder containers, the powders were sprayed in sequence, by following (Ni-20wt%Cr)6Al powders as a bond coat and finally Al<sub>2</sub>O<sub>3</sub>-3wtTiO<sub>2</sub> powder with particle size of -45+15µm as a top coating. In the spraying process, three passes were sprayed for (Ni-20%wtCr)6Al and 8 passes for Al<sub>2</sub>O<sub>3</sub>-3%wtTiO<sub>2</sub> coating. After coating, the samples were cooled in room temperature in order to avoid internal stress occurred to the coating. Finally, the samples were collected for analysis. Plasma primary and auxiliary gases were Ar and H<sub>2</sub>; N<sub>2</sub> was used as carrier gas. The substrates were stainless steel and prior to the plasma spraying, were degreased and grit blasted. The substrate was grit-blasted with corundum at a pressure of 3.2 bar and cleaned using ethanol in order to remove remaining dust or grease from the surface.

During the process, the material to be deposited is injected in powder form using argon as carrier gas. The main spraying parameters are listed in Table 1.

**Table 1.** Plasma spraying conditions

APS Parameters	Bond Coat	Powder Coating
Arc Current, A	600	650
Arc Voltage, V	60	50
Primary gas (Argon) flow rate	25	80 lpm
Secondary gas (He) flow rate	45	50 lpm
Powder carrier gas (Ar) flow rate	90	30 lpm
Powder flow rate	20	20 gpm
Spray distance	100	100 mm
Passes, layer	3	8
Spray angle, °	90°	90°

**Table 2.** chemical composition of AISI 304

Elements	C	Si	Mn	P	S	Cr	Ni	Co	Cu	Fe
% wt	0.032	0.75	2.00	0.045	0.030	17.5/19.5	8.0-10.5	0.122	0.375	Bal

## 2.2. Coating Characterization

The phase and microstructure analysis of the coating samples were measured using XRD Machine and Scanning Electron Microscopy (SEM). The wear tests were carried out on a sliding, reciprocating and vibrating test machine (SRV). The wear test mode is the reciprocal motion of a steel ball against a disc, as illustrated in Fig.1. The upper ball specimen bearing a normal load vibrates against the lower stationary disc specimen. The wear tests were performed under four applied loads (20, 40, 60 and 80 N), with a slip amplitude of 1.4 mm, a frequency of 30 Hz and a period of 20 min. For all wear experiments, the samples were unlubricated; the tests were conducted at an ambient temperature of 10oC and relative humidity of 60 ~ 70 %. The ball specimens were composed of steel with a diameter of 10 mm and the disc specimen were Al<sub>2</sub>O<sub>3</sub>-3wt% TiO<sub>2</sub> coated steel substrates with dimensions of 20x20x5 mm.

## 3. Results & Discussion

### 3.1. Morphology and structure

The samples with different setting parameters were observed for the coating morphology. Fig.2 shows an example of morphology of coated samples of coating surface. The coating features observe the molten particles condition and spread as out on top of the surface to develop coating layers. Some areas on the surface appear as semi-molten particles and they agglomerate together with molten particle to

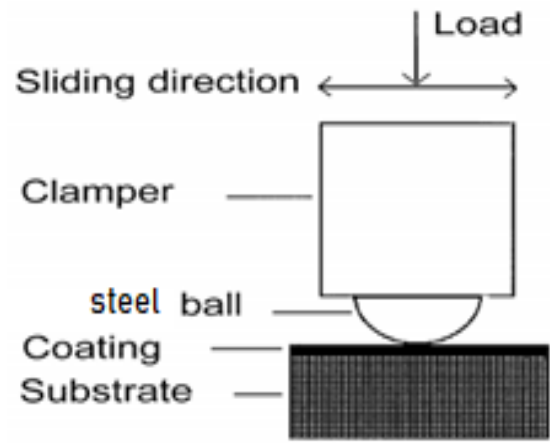


**Figure 1.** The schematic diagram of the SRV tester.

form coating layers [2,8,9]. The semi-molten particles exhibit pinholes, which are characteristic of porosity, occurred on the coated sample. The occurred porosity also may be due to the lamellae structure, which exhibit molten and semi-molten particles and will create pinholes inside the coating. The porosity may occur due to absorbed gases during spraying process. In this study, it is identified that the average porosity of the coating samples are 8.1%. Less porosity will produce better structure and bonding between the individual layers of coating. It also results in increase of density, hardness, adhesion strength and wear resistance of the coating [10,11].

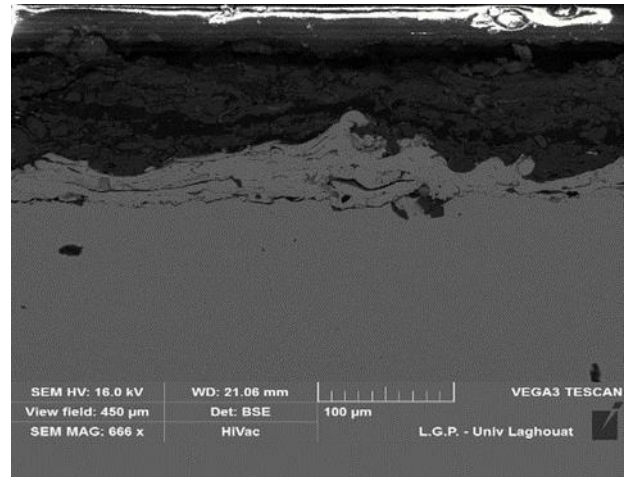


**Figure 2.** The morphology of coating surface scanning with SEM at magnification 100µm.

Referring to the coating cross-section samples, three different phases are observed. These are the Al<sub>2</sub>O<sub>3</sub>-3wt%TiO<sub>2</sub> coating (top coating), Ni-20wt%Cr6Al coating (bond coating) and metal substrate, which is shown in Fig.3.

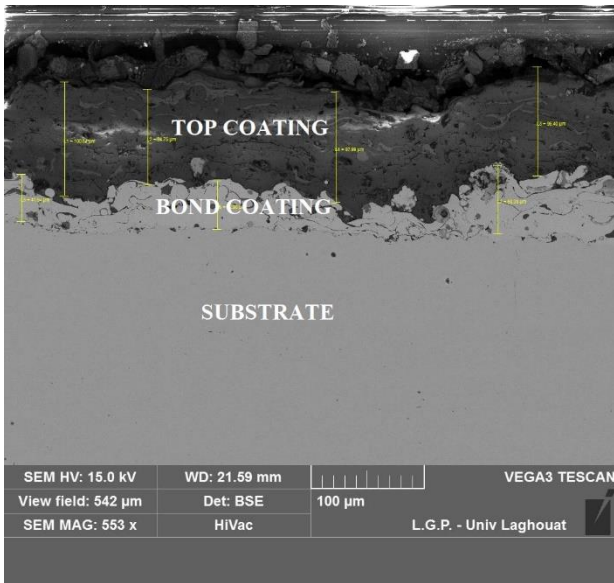


Figure 3. SEM micrographs of  $Al_2O_3$ -3wt.% $TiO_2$  coating at magnification  $200\mu m$ .

When the molten particle of  $Al_2O_3$ -3wt% $TiO_2$  impacted the substrate, it spreads and solidifies rapidly and formed a coating. The bonding effect of particles in forming a coating is due to mechanical interlocking, chemical reaction and partial fusion of the contact surface and will lead to mechanical adherence.

As shown in Fig.4, all  $Al_2O_3$ -3wt% $TiO_2$  coating predominately contains  $\gamma$ - $Al_2O_3$  (Gamma alumina) coexisting with  $\alpha$ - $Al_2O_3$ . In view of the nucleation kinetics, under-cooling of the  $\alpha$ - $Al_2O_3$  phase, resulting liquid droplets led to the nucleation of  $\gamma$ - $Al_2O_3$  nucleated rather than of  $\alpha$ - $Al_2O_3$ . This occurs because of lower interfacial energy between crystal and liquid [12]. Cooling rate after solidification was rapid enough to prevent subsequent transformation to  $\alpha$ - $Al_2O_3$ . The presence of  $\alpha$ - $Al_2O_3$  in the  $Al_2O_3$ -3wt% $TiO_2$  coating is due to the incorporation of unmelted particles during coating process [10,11].

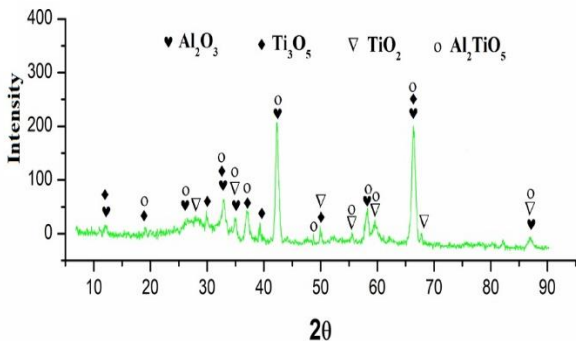


Figure 4. Typical Photo Of The XRD Patterns.

### 3.2. Wear and Friction

Fig.5 show the effect of contact load on the wear rate of the nanostructured  $Al_2O_3$ -3wt% $TiO_2$  coatings. The wear rate of the samples was lowest

at 20N and gradually increased with increasing load. The improved wear resistance of the coating was attributed to the increase of toughness and cohesion strength between splats [12,13].

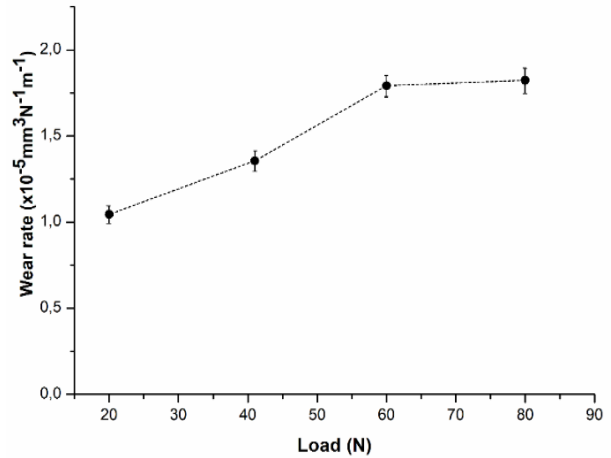


Figure 5. Wear rates of the sprayed  $Al_2O_3$ -3wt%  $TiO_2$  coatings sliding against steel ball

Fig.6 shows the steady-state friction coefficients of the nanostructured and conventional  $Al_2O_3$ -3wt%  $TiO_2$  coatings against a steel ball under dry sliding conditions. The results showed that the friction coefficients of coatings were similar at all test loads and exhibited no great change with increasing contact load under unlubricated conditions. The friction coefficients of the  $Al_2O_3$ -3wt.% $TiO_2$  coatings were similar and about 0.51.

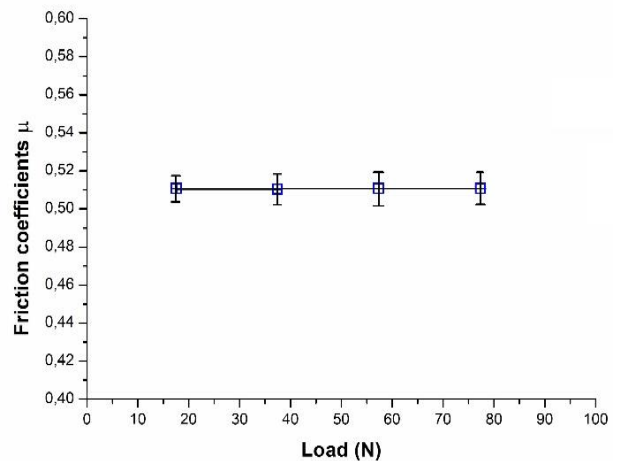


Figure 6. Friction coefficient of  $Al_2O_3$ -3wt%  $TiO_2$  coatings sliding against steel ball.

### 4. Conclusions

$Al_2O_3$ -3wt.% $TiO_2$  coatings were deposited by atmospheric plasma spraying. Microstructure and phase properties of the as-sprayed coatings were characterized.

The difference in microstructure and properties of the coatings led to different tribological behaviours.

The Al<sub>2</sub>O<sub>3</sub>-3wt.% TiO<sub>2</sub> coatings contained both equiaxed  $\alpha$ -Al<sub>2</sub>O<sub>3</sub> and  $\gamma$ -Al<sub>2</sub>O<sub>3</sub>. Moreover, the coating possessed a more homogeneous microstructure and TiO<sub>2</sub> phases is rutile in this coating, which is due to the reaction between TiO<sub>2</sub> and Al<sub>2</sub>O<sub>3</sub> particles during plasma spraying.

In addition, the coating possessed an improved wear resistance; it was gradually increased with increasing load. Although the friction coefficient exhibited no variation with increasing contact load.

### Acknowledgement

Authors gratefully thank Professor İskender Akkurt and other staff members of ICCESSEN 2019 for the best organization.

We gratefully thank Professor Omar Alaoui for his support, his useful and very important comments and for providing facilities in Process Engineering Laboratory, University of Laghouat for this study.

### References

- [1] L. Pawlowsky, *The Science and Engineering of Thermal Spray Coatings*, John Wiley & Sons, New York, 1995.
- [2] P. Fauchais, A. Vardelle, B. Dussoubs, in: *Thermal Spray 2001: New Surfaces for a New Millennium*, Eds. C.C. Berndt, K.A. Khor, E.F. Lugscheider, ASM International, Materials Park (OH) 2001, p. 1.
- [3] M. Djendel, O. Allaoui, R. Boubaaya, *Characterization of Alumina–Titania Coatings Produced by Atmospheric Plasma Spraying on 304 SS Steel*. *Acta Phys. Pol. A* 132, 538 Vol. 132(2017), DOI: 10.12693/APhysPolA.132.538
- [4] Günen, Ali. (2016). *Micro-Abrasion Wear Behavior of Thermal-Spray-Coated Steel Tooth Drill Bits*. *Acta Physica Polonica A*, DOI: 10.12693/APhysPolA.130.217
- [5] H. Ageorges, P. Ctibor, *Comparison of the structure and wear resistance of Al<sub>2</sub>O<sub>3</sub>–13wt.% TiO<sub>2</sub> coatings made by GSP and WSP plasma process with two different powders*, *Surf. Coat. Technol.* 202 (18) (2008) 4362–4368. DOI: 10.1016/j.surfcoat.2008.04.010
- [6] L. Shaw, D. Goberman, M. Gell, S. Jiang, Y. Wang, T.D. Xiao, P. Strutt, *The dependency of microstructure and properties of nanostructured coatings on plasma spray conditions*, *Surf. Coat. Technol.* 130 (2000) 1–8. DOI: 10.1016/S0257-8972(00)00673-3
- [7] E.H. Jordan, M. Gell, Y.H. Sohn, D. Goberman, L. Shaw, S. Jiang, M. Wang, T.D. Xiao, Y. Wang, P. Strutt, *Fabrication and evaluation of plasma sprayed nanostructured Alumina–Titania coatings with superior properties*, *Mater. Sci. Eng. A301* (2001) 80–89, [https://doi.org/10.1016/S0921-5093\(00\)01382-4](https://doi.org/10.1016/S0921-5093(00)01382-4)
- [8] İ.H. Karahan, *Effect of Borax Pentahydrate Addition to Acid Bath on the Microstructure and Corrosion Resistance of Zn-Co Coating*. *Acta Phys. Pol. A* Vol.128, B-432 (2015). DOI: 10.12693/APhysPolA.128.B-432
- [9] Djeghdjough Mohamed, Bacha Nacer eddine and Dilmi Nacer, *Effect of Substrate Preheating, Roughness and Particles Size on Splat Morphology of Thermal Sprayed Coatings*. *Proc. International Conference on Computational and Experimental Science and Engineering (IJCESEN)* Vol. 1-No.1 pp. 16-18(2015).
- [10] Rahim, M.S.A., Hayati, S.N. and Bakir, H.L. (2009) ‘Plasma spray ceramic coating and measurement of developed coating behaviour’, *Int. J. Precision Technology*, Vol. 1, No. 2, pp.163–172. DOI: 10.1504/IJPTech.2009.026375
- [11] M. Djendel, O. Allaoui, Abderrazak Bouzid. *Effect of Air Plasma Spraying Parameters on the Quality of Coating*. *Proc. International Journal of Computational and experimental Science and Engineering (IJCESEN)* Vol.2 –No. 2 (2016)pp.1-5.
- [12] Lin, X., Zeng, Y. and Ding, C.X. (2003) ‘Microstructure of alumina -3wt.% titania coating by plasma spraying with nanostructure powders’, *Materials Science and Engineering*, Vol.A.357, pp.228.234, [https://doi.org/10.1016/S0955-2219\(03\)00254-1](https://doi.org/10.1016/S0955-2219(03)00254-1)
- [13] Haghightzadeh, Azadeh & Mazinani, Babak & abdoahpour salari, Maryam. (2017). *Coating of Ordered Large-Pore Mesoporous Silica with TiO<sub>2</sub> Nanoparticles and Evaluation of Its Photocatalytic Activity*. *Acta Physica Polonica A*. DOI: 10.12693/APhysPolA.132.420.